Biodesign

pISSN 2288-6982 | eISSN 2288-7105

CRYSTALLIZATION P 92-95

Crystallization and preliminary X-ray analysis of API5–FGF2 complex

Seoung Min Bong[1] and Byung Il Lee[1,2,*]

[1]Research institute, National Cancer Center, Goyang-si, Gyeonggi 10408, Republic of Korea, [2]National Cancer Center Graduate School of Cancer Science and Policy, Goyang-si, Gyeonggi 10408, Republic

*Correspondence: bilee@ncc.re.kr

API5 is a unique oncogenic, non-BIR type IAP nuclear protein and is up-regulated in several cancers. It exerts several functions, such as apoptosis inhibition, cell cycle progression, cancer immune escape, and anticancer drug resistance. Although structural studies of API have revealed that API5 mediates protein-protein interactions, its detailed molecular functions remain unknown. Since FGF2 is one of API5's major interacting proteins, structural studies of the API5–FGF2 complex will provide insight into both proteins' molecular function. We overexpressed and purified API5 and FGF2 in *Escherichia coli* and crystallized the API–FGF2 complex using polyethylene glycol (PEG) 6000 as a precipitant. Diffraction data were collected to a 2.7 Å resolution using synchrotron X-rays. Preliminary diffraction analysis revealed that the API5–FGF2 complex crystal belongs to the space group $P2_12_12_1$ with the following unit cell parameters: a = 46.862, b = 76.523, c = 208.161 Å. One asymmetric unit with 49.9% solvent contains one API5-FGF2 complex. Molecular replacement calculation, using API5 and FGF2 coordinates, provided a clear electron density map for an API5–FGF2 complex.

INTRODUCTION

Apoptosis, a strictly regulated and programmed cell death, plays a key role in cell homeostasis (Hassan et al., 2014). Apoptosis signals occur along two pathways: a death-receptor-mediated extrinsic pathway, which engages cell surface death receptors by specific ligands; and a mitochondrial intrinsic pathway, which changes internal cellular integrity (de Almagro and Vucic, 2012; Vucic and Fairbrother, 2007). Defective apoptosis may cause several human disorders, including cancer, neurodegeneration, and autoimmune diseases (Hassan et al., 2014; Vucic and Fairbrother, 2007).

Inhibitor of apoptosis (IAP) proteins are major regulators of cell survival. They act by blocking apoptosis, modulating signal transduction, and affecting cell proliferation (de Almagro and Vucic, 2012; Dynek and Vucic, 2013; Vucic and Fairbrother, 2007). There are eight human IAP proteins (NAIP, c-IAP1-2, XIAP, surviving, Apollon/Bruce, ML-IAP, ILP-2), which are composed of a baculovirus IAP repeat (BIR) domain, a Ring domain (a really interesting new gene), a UBC (ubiquitin conjugating domain) and/or a CARD (caspase recruitment domain) (Dynek and Vucic, 2013).

Apoptosis Inhibitor 5 (API5), also known as AAC-11 (anti-apoptosis clone 11) or FIF (fibroblast growth factor 2-interacting factor), is a nuclear protein. Its expression prevents apoptosis under serum deprivation conditions (Tewari et al., 1997). Its expression is associated with tumor progression and with the malignant phenotype of tumor cells in several human cancers, such as cervical, lung, and B cell chromic lymphoid leukemia (Cho et al., 2014; Krejci et al., 2007; Sasaki et al., 2001). API5 suppresses E2F-dependent apoptosis, increases tumor cells' metastatic capacity by up-regulating MMP levels, via Erk signaling, and regulates cell cycle (Garcia-Jove Navarro et al., 2013; Morris et al., 2006; Song et al., 2015). API5 structural studies revealed it functions as a protein-protein interaction module (Han et al., 2012), and its identified binding partners include fibroblast growth factor 2 (FGF2), acinus, nucleoprotein (NP) of influenza A virus, estrogen receptor α, and caspase 2 (Basset et al., 2017; Imre et al., 2017; Mayank et al., 2015; Rigou et al., 2009; Van den Berghe et al., 2000).

Among the API5 binding partners, a fraction of FGF2 exists in the nucleus (Chlebova et al., 2009) and plays an important role in the tumorigenesis and angiogenesis of various tumors (Boelaert et al., 2003; Fukui et al., 2003). The smallest FGF2 variant, the18kDa low molecular weight (LMW) FGF2, is usually secreted by the cells and activated through binding with the cell surface FGF-receptor and heparin. FGF2 isoforms, which have a high molecular weight (HMW: 22, 22.5, 24, and 34 kDa), are usually localized in the nucleus, where they exert their functions (Chlebova et al., 2009). A fraction of LMW FGF2 can also exist in the nucleus. Although several studies have focused on secretory FGF2, detailed molecular functions of nuclear FGF2 remain to be elucidated.

Previous biochemical and structural studies on API5 and FGF2 have been insufficient to explain molecular function of these proteins. To understand the role of human API5 and FGF2 in the nucleus, we overexpressed and crystallized the human API5–FGF2 complex and determined its three-dimensional structure.

RESULTS AND DISCUSSION

API5 and FGF2 genes were subcloned into *E. coli* expression vectors for protein overexpression (Table 1). The resulting proteins, which contained polyhistidine tags at their N-terminus, were used for protein purification. Both proteins were purified separately by Ni-NTA affinity column chromatography and size-exclusion chromatography (SEC). The final yields of API5 and FGF2 were 15.5 mg and 5.3 mg per liter of cell culture, respectively. The API5 and FGF2 proteins presented molecular weights of 59 kDa and 17 kDa, respectively. The size and purity of purified recombinant API5 and FGF2 proteins were analyzed by SDS-PAGE (Figure 1A). In the SEC step, API5's elution peak profile showed a single peak and was eluted at a 78 ml volume, which, based on the molecular weight standard, represented a molecular weight of approximately 60 kDa (Figure 1B). FGF2 presented three peaks on the SEC elution profile. It existed in the final peak and eluted at an 80 ml volume, which, based on the molecular weight standard, corresponds to an apparent molecular weight of 17 kDa (Figure 1C). This indicates that, in solution, API5 and FGF2 exist as monomers.

TABLE 1 | Macromolecule-production information

Source organism	Homo sapiens
DNA source	UniProtKB-Q9BZZ5 (API5) Codon optimized (synthesized) FGF2
Expression vector	pET-28b(+)_API5 pHis_FGF2 (modified version of pET-28)
Expression host	*E. coli* Rosetta2 (DE3)
Complete amino-acid sequence of the construct produced	>API5(1-504) MGSSHHHHHHSSGLVPRGSHMPTVEELYRNYGILA DATEQVGQHKDAYQVILDGVKGGTKEKRLAAQFIPK FFKHFPELADSAINAQLDLCEDEDVSIRRQAIKELPQ FATGENLPRVADILTQLLQTDDSAEFNLVNNALLSIFK MDAKGTLGGLFSQILQGEDIVRERAIKFLSTKLKTLP DEVLTKEVEELILTESKKVLEDVTGEEFVLFMKILSGL KSLQTVSGRQQLVELVAEQADLEQTFNPSDPDCVD RLLQCTRQAVPLFSKNVHSTRFVTYFCEQVLPNLG TLTTPVEGLDIQLEVLKLLAEMSSFCGDMEKLETNLR KLFDKLLEYMPLPPEEAENGENAGNEEPKLQFSYVE CLLYSFHQLGRKLPDFLTAKLNAEKLKDFKIRLQYFA RGLQVYIRQLRLALQGKTGEALKTEENKIKVVALKITN NINVLIKDLFHIPPSYKSTVTLSWKPVQKVEIGQKRAS EDTTSGSPPKKSSAGPKRDARQIYNPPSGKYSSNL GNFNYEQRGAFRGSRGGRGWGTRGNRSRGRLY >FGF2 (135-288; C211S and C229S are colored in red) MHHHHHHGSLVPRSENLYFQGSAAGSITTLPALPED GGSGAFPPGHFKDPKRLYCKNGGFFLRIHPDGRVD GVREKSDPHIKLQLQAEERGVVSIKGVSANRYLAMK EDGRLLASKSVTDECFFFERLESNNYNTYRSRKYTS WYVALKRTGQYKLGSKTGPGQKAILFLPMSAKS

The underlined characters in amino acid sequences are cloning artifacts for affinity tag and protease cleavage.

API5–FGF2 complex crystals were found under various crystallization conditions. The best crystals were obtained using a reservoir solution of 100 mM Na-HEPES pH 7.5, 100 mM KCl, and 10% (v/v) polyethylene glycol (PEG) 6,000 (Figure 2, Table 2). X-ray diffraction data of the complex crystal was collected to 2.7 Å resolution on the Beamline 7A at the Pohang Accelerator Laboratory (Pohang, Republic of Korea) (Figure 3). The API5–FGF2 complex crystal belonged to the orthorhombic space group $P2_12_12_1$ with the following unit cell parameters: a = 46.862, b = 76.523, c = 208.161 Å (Table 3). The calculated Matthews coefficient (V_M) value was 2.46 $Å^3$ Da^{-1} and the solvent content was about 49.9% in volume (Matthews, 1968). Asymmetric unit contains one API5-FGF2 complex. The phase problem was solved using the molecular replacement method with the previously reported structures of API5 (PDB code: 3U0R) and FGF2 (PDB code: 1BAS) (Han et al., 2012; Zhu et al., 1991). Each API5 and FGF2 molecule was identified by interpreting the resulting electron density maps (Figure 4). Initial R_{work} and R_{free} values were calculated to be 24.1 and 29.2%, respectively.

METHODS

Gene cloning

The DNA constructs of full length API5 (1–504, isoform 2) and FGF2 (135–280; C211S/ C229S) were amplified by polymerase chain reaction. For

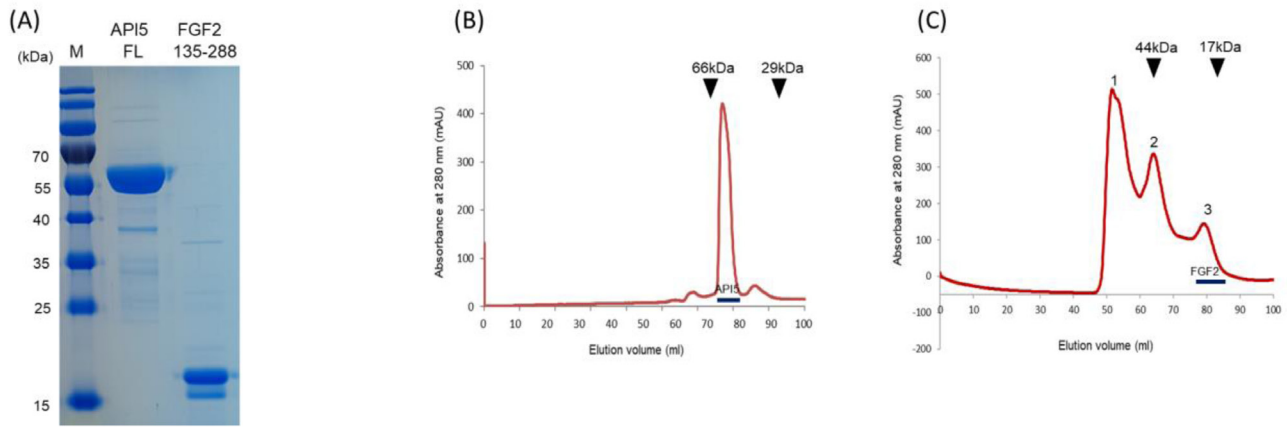

FIGURE 1 | **Purification of API5 and FGF2.** (A) SDS-PAGE analysis of the API5 and FGF2 proteins, compared to molecular weight standards. (B) API5 SEC profile. The standards were calibrated using albumin (66 kDa) and carbonic anhydrase (29 kDa), as indicated above the SEC profile. (C) FGF2 SEC profile. The standards were calibrated using Ovalbumin (44 kDa) and Myoglobulin (17 kDa), as indicated above the SEC profile. The chromatogram for FGF2 contains three peaks (peak 1, high molecular weight aggregated FGF2; peak 2, dimer size FGF2; peak 3, monomer size FGF2).

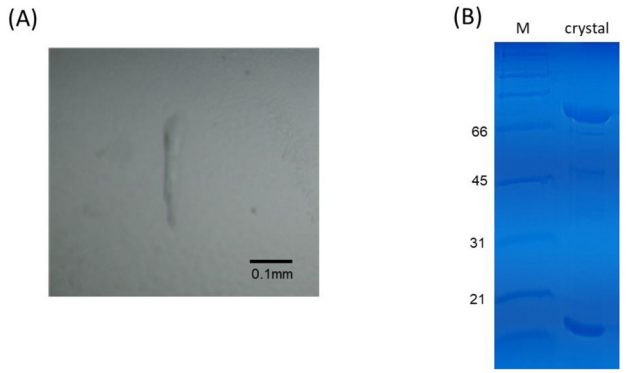

FIGURE 2 | (A) An API5–FGF2 complex crystal. The scale bar is presented in the right bottom side. (B) SDS-PAGE gel image of the crystal.

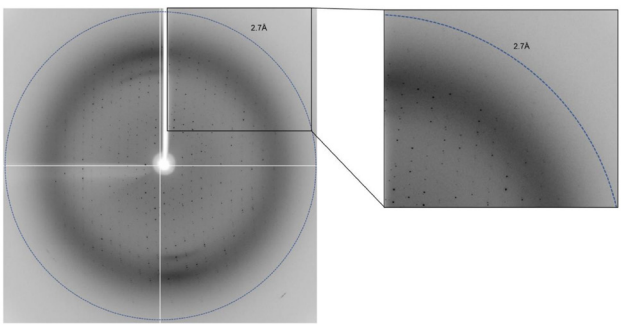

FIGURE 3 | Representative X-ray diffraction image of the API5–FGF2 complex crystal. Resolution circles are shown.

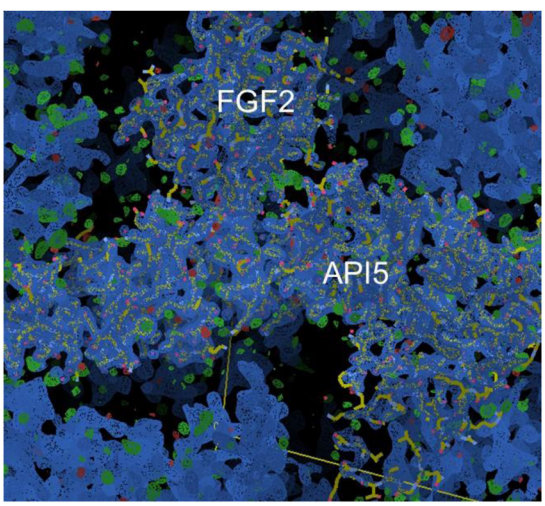

FIGURE 4 | Electron density maps (Blue, 2mFo-DFcalc; Green, mFo-DFcalc) after molecular replacement phase calculation.

FGF2, two cysteine residues in the disulfide bond formation were replaced with serine. The amplified API5 and FGF2 (135–280) DNA fragments were then inserted into the expression vector pET-28b(+), using the NdeI/NotI restriction enzyme sites, and into the modified pET-28 vector (Novagen, USA) using the BamHI/EcoRI restriction enzyme sites for expression of N-terminal polyhistidine-tagged proteins (Table 1).

TABLE 2 | Crystallization

Method	Sitting-drop vapor diffusion
Plate type	MRC 96-well plate
Temperature (K)	277
Protein concentration (mg/ml)	3.875 and 3.975 (API5 and FGF2, respectively)
Buffer composition of protein solution	20 mM Tris-HCl pH 7.5, 200 mM NaCl, and 1 mM 1,4-dithiothreitol
Composition of reservoir solution	100 mM Na-HEPES pH 7.5, 100 mM KCl, and 10% (v/v) PEG 6,000
Volume (μl) and ratio of drop	2 (1:1 ratio of protein and reservoir)
Volume of reservoir (μl)	70

TABLE 3 | Data collection and refinement statistics

X-ray source	PLS-7A
X-ray wavelength (Å)	1.000
Space group	$P2_12_12_1$
Unit cell parameters (Å)	a=46.862, b=76.523, c=208.161
Resolution range (Å)	50.0-2.7 (2.75-2.70)
Total/unique reflections	96,323/20,633
Completeness (%)	95.2 (82.4)
I/σI	17.8 (2.4)
R_{merge} (%)	10.3 (36.8)
Redundancy	4.7 (2.8)

Value in parentheses are for highest-resolution shell.

Recombinant protein expression and purification

The proteins were overexpressed in the *Escherichia coli* Rosetta2 (DE3) strain (Novagen, USA). Recombinant proteins were induced using 0.5 mM isopropyl-β-D-thiogalactopyranoside at 37°C for API5 and 18°C for FGF2, and the cells were further cultured for 4 and 20 hours, respectively. Each protein pellet was resuspended in an ice-cold lysis buffer (20 mM Tris-HCl pH 7.5, 350 mM NaCl, 2 mM KCl, 10% glycerol, and 1 mM phenylmethylsulfonyl fluoride), and the cells were disrupted by sonication. Crude lysates were centrifuged at 13,000 g for 1 hour at 4°C. Supernatants were loaded onto an Ni-NTA Agarose (Qiagen, Germany), using open column, pre-equilibrated with binding buffer (20 mM Tris-HCl pH 7.5, 350 mM NaCl, 2 mM KCl, 10% glycerol) and subsequently washed with washing buffer (20 mM Tris-HCl pH 7.5, 350 mM NaCl, 2 mM KCl, 10% glycerol, and 30 mM imidazole). The proteins were eluted with elution buffer (20 mM Tris-HCl pH 7.5, 350 mM NaCl, 2 mM KCl, 10% glycerol, and 300 mM imidazole), and the eluents were subsequently applied into a HiLoad 16/600 superdex 200 prep grade column (GE Healthcare, USA) for API5 or a HiLoad 16/600 superdex 75 for FGF2, both pre-equilibrated with buffer containing 20 mM Tris-HCl pH 7.5, 200 mM NaCl, and 1 mM 1,4-dithiothreitol. Both purified proteins were concentrated to 15.5 mg ml^{-1} and 5.3 mg ml^{-1} using an Amicon Ultra-15 ultrafiltration device (Millipore, Germany) for structural studies. The protein concentration was determined using the Bradford method with bovine serum albumin as standard.

Crystallization and x-ray data collection

The API5–FGF2 complex was assembled by mixing the purified API5 (100 μl of 15.5 mg ml^{-1}) with FGF2 (300 μl of 5.3 mg ml^{-1}) and storing the mixture at 4°C, overnight. The molar ratio between API5 and FGF2 was 1:3. Initial crystallization screening was performed via the sitting-

drop vapor diffusion method in 96-well plates at 4°C, using commercially available crystallization kits. Crystals were obtained in a reservoir solution of 100 mM Na-HEPES pH 7.5, 100 mM KCl, and 10% (v/v) PEG 6,000. Crystallization drops were prepared by mixing 1 μl of purified protein with 1 μl of reservoir solution. Before flash-freezing in liquid nitrogen, the crystal was transferred into the reservoir solution supplemented with 10% (v/v) PEG 400. X-ray diffraction data were collected using an ADSC Q270 detector at the beamline 7A of Pohang Light Source (Pohang, Korea). A total range of 200° was covered with 1.0° oscillation. The synchrotron X-rays' wavelength was 1.000 Å, and the crystal-to-detector distance was 300 mm. Diffraction data were collected to 2.7 Å from a native crystal. Raw data were processed and scaled using the HKL2000 software package (Otwinowski and Minor, 1997).

CONFLICT OF INTEREST

The authors declare no potential conflicts of interest.

ACKNOWLEDGEMENTS

We thank the beamline staff of Pohang Light Source (Beamline 7A) for assistance with X-ray data collection. This work was partially supported by a National Cancer Center Research Grant (1831120 to B.I.L.) and National Research Foundation of Korea (NRF) grants funded by the Korea government (MSIT) (NRF-2018R1A5A2023127 and NRF-2015R1A2A2A01003004 to B.I.L.).

Original Submission: Oct 5, 2018
Revised Version Received: Oct 24, 2018
Accepted: Oct 25, 2018

REFERENCE

Basset, C., Bonnet-Magnaval, F., Navarro, M.G., Touriol, C., Courtade, M., Prats, H., Garmy-Susini, B., and Lacazette, E. (2017). Api5 a new cofactor of estrogen receptor alpha involved in breast cancer outcome. *Oncotarget* **8**, 52511-52526.

Boelaert, K., McCabe, C.J., Tannahill, L.A., Gittoes, N.J., Holder, R.L., Watkinson, J.C., Bradwell, A.R., Sheppard, M.C., and Franklyn, J.A. (2003). Pituitary tumor transforming gene and fibroblast growth factor-2 expression: potential prognostic indicators in differentiated thyroid cancer. *J Clin Endocrinol Metab* **88**, 2341-2347.

Chlebova, K., Bryja, V., Dvorak, P., Kozubik, A., Wilcox, W.R., and Krejci, P. (2009). High molecular weight FGF2: the biology of a nuclear growth factor. *Cell Mol Life Sci* **66**, 225-235.

Cho, H., Chung, J.Y., Song, K.H., Noh, K.H., Kim, B.W., Chung, E.J., Ylaya, K., Kim, J.H., Kim, T.W., Hewitt, S.M., and Kim, J.H. (2014). Apoptosis inhibitor-5 overexpression is associated with tumor progression and poor prognosis in patients with cervical cancer. *BMC Cancer* **14**, 545.

de Almagro, M.C., and Vucic, D. (2012). The inhibitor of apoptosis (IAP) proteins are critical regulators of signaling pathways and targets for anti-cancer therapy. *Exp Oncol* **34**, 200-211.

Dynek, J.N., and Vucic, D. (2013). Antagonists of IAP proteins as cancer therapeutics. *Cancer Lett* **332**, 206-214.

Fukui, S., Nawashiro, H., Otani, N., Ooigawa, H., Nomura, N., Yano, A., Miyazawa, T., Ohnuki, A., Tsuzuki, N., Katoh, H., Ishihara, S., and Shima, K. (2003). Nuclear accumulation of basic fibroblast growth factor in human astrocytic tumors. *Cancer* **97**, 3061-3067.

Garcia-Jove Navarro, M., Basset, C., Arcondeguy, T., Touriol, C., Perez, G., Prats, H., and Lacazette, E. (2013). Api5 contributes to E2F1 control of the G1/S cell cycle phase transition. *PLoS One* **8**, e71443.

Han, B.G., Kim, K.H., Lee, S.J., Jeong, K.C., Cho, J.W., Noh, K.H., Kim, T.W., Kim, S.J., Yoon, H.J., Suh, S.W., Lee, S., and Lee, B.I. (2012). Helical repeat structure of apoptosis inhibitor 5 reveals protein-protein interaction modules. *J Biol Chem* **287**, 10727-10737.

Hassan, M., Watari, H., AbuAlmaaty, A., Ohba, Y., and Sakuragi, N. (2014). Apoptosis and molecular targeting therapy in cancer. *Biomed Res Int* **2014**, 150845.

Imre, G., Berthelet, J., Heering, J., Kehrloesser, S., Melzer, I.M., Lee, B.I., Thiede, B., Dotsch, V., and Rajalingam, K. (2017). Apoptosis inhibitor 5 is an endogenous inhibitor of caspase-2. *EMBO Rep* **18**, 733-744.

Krejci, P., Pejchalova, K., Rosenbloom, B.E., Rosenfelt, F.P., Tran, E.L., Laurell, H., and Wilcox, W.R. (2007). The antiapoptotic protein Api5 and its partner, high molecular weight FGF2, are up-regulated in B cell chronic lymphoid leukemia. *J Leukoc Biol* **82**, 1363-1364.

Matthews, B.W. (1968). Solvent content of protein crystals. *J Mol Biol* **33**, 491-497.

Mayank, A.K., Sharma, S., Nailwal, H., and Lal, S.K. (2015). Nucleoprotein of influenza A virus negatively impacts antiapoptotic protein API5 to enhance E2F1-dependent apoptosis and virus replication. *Cell Death Dis* **6**, e2018.

Morris, E.J., Michaud, W.A., Ji, J.Y., Moon, N.S., Rocco, J.W., and Dyson, N.J. (2006). Functional identification of Api5 as a suppressor of E2F-dependent apoptosis in vivo. *PLoS Genet* **2**, e196.

Otwinowski, Z., and Minor, W. (1997). Processing of X-ray diffraction data collected in oscillation mode. *Methods Enzymol* **276**, 307-326.

Rigou, P., Piddubnyak, V., Faye, A., Rain, J.C., Michel, L., Calvo, F., and Poyet, J.L. (2009). The antiapoptotic protein AAC-11 interacts with and regulates Acinus-mediated DNA fragmentation. *EMBO J* **28**, 1576-1588.

Sasaki, H., Moriyama, S., Yukiue, H., Kobayashi, Y., Nakashima, Y., Kaji, M., Fukai, I., Kiriyama, M., Yamakawa, Y., and Fujii, Y. (2001). Expression of the antiapoptosis gene, AAC-11, as a prognosis marker in non-small cell lung cancer. *Lung Cancer* **34**, 53-57.

Song, K.H., Kim, S.H., Noh, K.H., Bae, H.C., Kim, J.H., Lee, H.J., Song, J., Kang, T.H., Kim, D.W., Oh, S.J., Jeon, J.H., and Kim, T.W. (2015). Apoptosis Inhibitor 5 Increases Metastasis via Erk-mediated MMP expression. *BMB Rep* **48**, 330-335.

Tewari, M., Yu, M., Ross, B., Dean, C., Giordano, A., and Rubin, R. (1997). AAC-11, a novel cDNA that inhibits apoptosis after growth factor withdrawal. *Cancer Res* **57**, 4063-4069.

Van den Berghe, L., Laurell, H., Huez, I., Zanibellato, C., Prats, H., and Bugler, B. (2000). FIF [fibroblast growth factor-2 (FGF-2)-interacting-factor], a nuclear putatively antiapoptotic factor, interacts specifically with FGF-2. *Mol Endocrinol* **14**, 1709-1724.

Vucic, D., and Fairbrother, W.J. (2007). The inhibitor of apoptosis proteins as therapeutic targets in cancer. *Clin Cancer Res* **13**, 5995-6000.

Zhu, X., Komiya, H., Chirino, A., Faham, S., Fox, G.M., Arakawa, T., Hsu, B.T., and Rees, D.C. (1991). Three-dimensional structures of acidic and basic fibroblast growth factors. *Science* **251**, 90-93.